

Optimized operation of a controlled stirred tank reactor system for the production of mesenchymal stromal cells and their extracellular vesicles

Ana Fernandes-Platzgummer¹, Raquel Cunha¹, Sara Morini¹, Marta Carvalho¹, Juan Moreno-Cid², Joaquim Cabral¹, and Claudio Lobato da Silva¹

¹Universidade de Lisboa Instituto Superior Tecnico

²Bionet Servicios Técnicos SL

December 21, 2022

Abstract

The therapeutic effects of human mesenchymal stromal cells (MSC) have been attributed mostly to their paracrine activity, exerted through small-secreted extracellular vesicles (EVs) rather than their engraftment into injured tissues. Currently, the production of MSC-derived EVs (MSC-EVs) is performed in laborious static culture systems with limited manufacturing capacity using serum-containing media. In this work, a serum-/xenogeneic-free microcarrier-based culture system was successfully established for bone marrow-derived MSC cultivation and MSC-EV production using a 2 L-scale controlled stirred tank reactor (STR) operated under fed-batch (FB) or fed-batch combined with continuous perfusion (FB/CP). Overall, maximal cell numbers of $(3.0 \pm 0.12) \times 10^8$ and $(5.3 \pm 0.32) \times 10^8$ were attained at days 8 and 12 for FB and FB/CP cultures, respectively, and MSC(M) expanded under both conditions retained their immunophenotype. MSC-EVs were identified in the conditioned medium collected from all STR cultures by TEM, and EV protein markers were successfully identified by WB analysis. Overall, no significant differences were observed between EVs isolated from MSC expanded in STR operated under the two feeding approaches. EV mean sizes of 163 ± 5.27 nm and 162 ± 4.44 nm ($P > 0.05$) and concentrations of $(2.4 \pm 0.35) \times 10^{11}$ EVs/mL and $(3.0 \pm 0.48) \times 10^{11}$ EVs/mL ($P > 0.05$) were estimated by nanoparticle tracking analysis for FB and FB/CP cultures, respectively. The STR-based platform optimized herein represents a major contribution towards the development of human MSC- and MSC-EV-based products as promising therapeutic agents for Regenerative Medicine settings.

Ana Fernandes-Platzgummer^{1,2*}, Raquel Cunha^{1,2,α}, Sara Morini^{1,2,β}, Marta Carvalho^{1,2}, Juan Moreno-Cid³, Joaquim M.S. Cabral^{1,2}, Cláudia Lobato da Silva^{1,2}

1. Department of Bioengineering and iBB – Institute for Bioengineering and Biosciences, Instituto Superior Técnico, Universidade de Lisboa, Av. Rovisco Pais, 1049-001 Lisboa, Portugal
2. Associate Laboratory i4HB - Institute for Health and Bioeconomy, Instituto Superior Técnico, Universidade de Lisboa, Av. Rovisco Pais, 1049-001 Lisboa, Portugal
3. Bionet Servicios Técnicos S.L., Avenida Azul, parcela 2.11.2, 30320 Parque Tecnológico de Fuente Álamo (Murcia), CIF B73053423

* Corresponding author:

Ana Fernandes-Platzgummer

Address: Instituto Superior Técnico- Taguspark, Av. Prof. Dr. Cavaco Silva, 2744-016 Porto Salvo, Oeiras, Portugal

Phone number: +351 210407038

E-mail address: ana.fernandes@tecnico.ulisboa.pt

Short running title: Producing MSC and derived EVs in stirred tank reactors

Ana Fernandes-Platzgummer 0000-0002-5367-6528

Raquel Cunha 0000-0001-7935-188X

Marta Carvalho 0000-0003-1026-1995

Sara Morini 0000-0002-9124-1795

Juan Moreno-Cid 0000-0003-3187-3296

Joaquim M.S. Cabral <https://orcid.org/0000-0002-2405-5845>

Cláudia Lobato da Silva <https://orcid.org/0000-0002-1091-7651>

^αRaquel Cunha current affiliation: Clinical Academic Center (2CA-Braga), Braga, Portugal.

^βSara Morini current affiliation: Banc de Sang i Teixits, Edifici Dr. Frederic Duran i Jordà, Passeig Taulat, 116, 08005 Barcelona, Spain; and Musculoskeletal Tissue Engineering Group, Vall d’Hebron Research Institute (VHIR), Universitat Autònoma de Barcelona, Passeig de la Vall d’Hebron 129-139, 08035 Barcelona, Spain.

ABSTRACT

The therapeutic effects of human mesenchymal stromal cells (MSC) have been attributed mostly to their paracrine activity, exerted through small-secreted extracellular vesicles (EVs) rather than their engraftment into injured tissues. Currently, the production of MSC-derived EVs (MSC-EVs) is performed in laborious static culture systems with limited manufacturing capacity using serum-containing media. In this work, a serum-/xenogeneic-free microcarrier-based culture system was successfully established for bone marrow-derived MSC cultivation and MSC-EV production using a 2 L-scale controlled stirred tank reactor (STR) operated under fed-batch (FB) or fed-batch combined with continuous perfusion (FB/CP). Overall, maximal cell numbers of $(3.0 \pm 0.12) \times 10^8$ and $(5.3 \pm 0.32) \times 10^8$ were attained at days 8 and 12 for FB and FB/CP cultures, respectively, and MSC(M) expanded under both conditions retained their immunophenotype. MSC-EVs were identified in the conditioned medium collected from all STR cultures by TEM, and EV protein markers were successfully identified by WB analysis. Overall, no significant differences were observed between EVs isolated from MSC expanded in STR operated under the two feeding approaches. EV mean sizes of 163 ± 5.27 nm and 162 ± 4.44 nm ($P > 0.05$) and concentrations of $(2.4 \pm 0.35) \times 10^{11}$ EVs/mL and $(3.0 \pm 0.48) \times 10^{11}$ EVs/mL ($P > 0.05$) were estimated by nanoparticle tracking analysis for FB and FB/CP cultures, respectively. The STR-based platform optimized herein represents a major contribution towards the development of human MSC- and MSC-EV-based products as promising therapeutic agents for Regenerative Medicine settings.

Keywords

Ex vivo Expansion; Mesenchymal Stromal Cells; Extracellular Vesicles; stirred tank reactor; Feeding regime; continuous perfusion; Fed-batch

INTRODUCTION

In the last decades, human mesenchymal stromal cells (MSC) have emerged as a main player in the field of Regenerative Medicine. Up to 448 clinical trials with human MSC were running within phases I and II including 48 for the treatment of SARS-CoV-2 Induced Acute Respiratory Failure (www.clinicaltrials.gov, terms searched: “mesenchymal stromal cells”, “mesenchymal stem cells” and “mesenchymal stem/stromal cells”, December 2022). Human MSC have been defined as plastic adherent, fibroblast-like cells, expressing

cell surface markers such as CD73, CD90, CD105, CD29, CD44, CD49a-f, while being negative for CD14, CD19, CD34, CD45 and HLA-DR expression and can differentiate into multiple mesoderm-type cell lineages. These multipotent cells are present in several tissues including bone marrow (BM), adipose tissue (AT), Wharton’s jelly (WJ), dental pulp, synovial fluid, placenta, amniotic fluid and others. Due to their ability to home to injury sites and promote a regenerative microenvironment, combined with their multilineage differentiation potential, MSC have been widely employed in clinical trials for blood-related diseases (Le Blanc et al., 2008; Prasad et al., 2011), autoimmune diseases (Duijvestein et al., 2010; Garcia-Olmo et al., 2005; Mazzini et al., 2010) and tissue engineering (Horwitz et al., 2002; Horwitz et al., 1999), with encouraging results. More recently, these beneficial effects of human MSC have been attributed mostly to their paracrine activity, exerted through MSC-secreted modulating factors, rather than their engraftment into injured tissues (Kraitchman et al., 2005; Toma et al., 2009). Indeed, emerging evidence associates these paracrine effects to MSC-derived extracellular vesicles (EVs), which play a central role in cell-to-cell interaction and communication in a pleiotropic way (Balbi et al., 2017; Camussi et al., 2013; Zhang et al., 2014). The EVs released by the donor cells can be uptaken by nearby cells or distant cells, subsequently modulating recipient cells (Phinney & Pittenger, 2017). The universally used expression “EVs” comprises all vesicle subtypes (exosomes, microvesicles and apoptotic bodies) and is a highly heterogeneous pool concerning size range (30-5000 nm), origin, content (proteins, lipids, genetic material and organelles such as mitochondria), biochemical and biophysical features, and biological functions. Compared to cell therapies, the use of EVs as cell-free therapeutic products presents several potential advantages namely: (i) EVs are relatively safer, as they are completely non-replicative and not mutagenic (Elsharkasy et al., 2020); (ii) EVs have also a low risk of inducing microvasculature obstruction upon administration due to their smaller size; (iii) EVs have long circulating half-life and the ability to cross the blood brain barrier (BBB) (Cerri et al., 2015; Moon et al., 2019); (iv) EVs have a simpler composition than parental cells, although still complex and with a bioactive cargo; (v) EVs can be used as delivery systems with increased efficacy and homing capacity (de Almeida Fuzeta et al., 2022; Katsuda et al., 2013; Pascucci et al., 2014); (vi) EVs as non-living biological products are more resistant to manipulation than living cells; (vii) the possibility of using reduced doses *in vivo* to achieve a therapeutic response, as EVs can evade phagocytes (Baglio et al., 2015); and (viii) EVs can be potentially stored with no need of potentially toxic cryoprotectants at -20°C for six months without loss of their biochemical activity (Alvarez-Erviti et al., 2011; Sun et al., 2010; Webber & Clayton, 2013). Overall, the regulatory aspects for producing EV-based products for therapeutic strategies is expected to be less complicated than for any therapy based on *in vitro* expanded cells. Concerning their therapeutic use, EVs can be used as biomedicines, taking advantage of their natural intrinsic medicinal effects, which can be further improved by manipulating the parental cell towards the production of more specialized and efficient EVs (Fan et al., 2020; Haraszti et al., 2018). Alternatively, EVs can be used as drug delivery systems (DDS), by loading various types of therapeutics, including genetic material and drugs (Malhotra et al., 2019).

From a manufacturing perspective, EV production comprises, sequentially: culture of the parental cell line (i.e. MSC); their collection or harvest from the conditioned medium (i.e. culture supernatant); and purification. Until now, MSC-EV production have been performed using serum-containing media, mostly of animal origin, in planar systems under static conditions, which are limited in terms of cell productivity; their non-homogeneous nature results in concentration gradients (e.g. pH, metabolites); are difficult to monitor; and ultimately unsafe as animal-origin material represent a risk of microbial/prion contamination (Sotiropoulou et al., 2006). Moreover, since the concentration of MSC-EV in the conditioned medium is typically low, scale-out to hundreds of T-flasks or multiplate flask systems is required, involving an extensive handling for feeding/harvesting procedures, to achieve a significant final mass production. Additionally, several differences were observed, in terms of the MSC-derived EVs cargo, between EVs isolated from culture supernatants of MSC expanded under different culture conditions, stressing the importance of controlling all culture process parameters to obtain a consistent EV content (Hyland et al., 2020; Kay et al., 2021). In this context, it turns necessary to move forward to fully controlled reactors (i.e. stirred tank reactors (STR)) to establish a reproducible and scalable process to produce MSC-EV. In addition, the use of defined serum-/xenogeneic-free (S/X-free) culture medium formulations could result in substantial improvements for MSC-EV production in terms of reproducibility, stability and quality, while ensuring the approval of regulatory agencies. Besides pH,

dissolved oxygen and temperature, another important bioprocess parameter that is crucial to monitor and control during STR cultures is the nutrient/metabolite concentration profiles in culture. For that reason, it is important to design efficient feeding schemes able to maximize cell densities in a cost-effective way. Different strategies can be considered for human cell cultures: batch, where no culture medium is added or withdrawn during culture; fed-batch, where fresh culture medium is added discretely/continuously to the STR but no culture supernatant is withdrawn; and continuous perfusion operation with cell retention, where there is an automated continuous replenishment/removal of fresh/exhausted culture medium. Fed-batch is the feeding operation mode of choice in the pharmaceutical sector due to the high cell densities and consequently high product titers (e.g. antibodies) attained, as well as its simplicity, among other features. On the other hand, perfusion cultures allow higher cell productivities and a steady state operation, as well as better cell physiology control that is crucial when cells are the target product. As main disadvantages, perfusion cultures are generally more costly and sometimes difficult to implement, especially due to the cell retention device (e.g. continuous centrifuges, tangential flow membrane filters and spin-filters). In this work, a scalable S/X-free process to produce MSC and MSC-EVs in a fully controlled STR was successfully established. Two different feeding operation modes were compared in what concerns MSC yields and identity and EVs production: fed-batch (FB) and FB combined with continuous perfusion (CP). The use of FB followed by CP is expected to combine the advantages of the two processes, as no important autocrine factors are withdrawn from the STR during the first days, when the cell number is still low (FB process), and CP process, when the cell number increases and the need for culture medium exchange is deemed needed.

The manufacturing platform established herein is expected to pave a new way for the development of MSC-based therapies, eliminating time- and labour-consuming procedures aiming at the scalable production of well-defined MSC populations as well as their secreted EVs to boost their medical uses.

MATERIALS AND METHODS

2.1 Human cells

The human MSC derived from bone marrow [MSC(M)] used in this study are part of the cell bank available at the Stem Cell Engineering Research Group (SCERG), iBB-Institute for Bioengineering and Biosciences at Instituto Superior Técnico (IST). MSC were previously isolated/expanded according to protocols previously established at iBB-IST (Dos Santos et al., 2010). Bone marrow aspirates were obtained from IPO Lisboa from healthy donors after written informed consent according to the Directive 2004/23/EC of the European Parliament and of the Council of 31 March 2004 on setting standards of quality and safety for the donation, procurement, testing, processing, preservation, storage and distribution of human tissues and cells (Portuguese Law 22/2007, June 29), with the approval of the Ethics Committee of the respective clinical institution.

2.2 MSC(M) expansion under static conditions

Prior to bioreactor inoculation, cryopreserved MSC(M) were thawed and expanded at a cell density of 3000 cells/cm² with StemPro™ MSC SFM XenoFree supplemented with 1% (v/v) GlutaMAX™ and 1% (v/v) Antibiotic-Antimycotic (10,000 units/mL of penicillin, 10,000 µg/mL of streptomycin and 25 µg/mL of Amphotericin B) (StemPro culture medium) on pre-coated T-flasks with CELLstart™ Substrate [diluted 1:100 in phosphate buffered saline (PBS)]. At 70-80% cell confluence, MSC were detached from the flasks by adding TrypLE™ Select Enzyme (diluted 1:10 in PBS) for 7 min at 37°C. Cell number and viability were determined using the Trypan Blue exclusion method. All reagents were acquired from Gibco™, Thermo Fisher Scientific, USA.

2.3 MSC(M) expansion under stirred conditions

Non-porous SoloHill® plastic microcarriers (Sartorius, Germany) were prepared according to manufacturer's instructions. Briefly, 20 g of plastic microcarriers were autoclaved at 121°C for 20 minutes, washed once with

PBS and coated with CELLstart™ Substrate (diluted 1:100 in PBS) for 2 h at 37°C, using a 250 mL Bellco spinner flask (Bellco Glass, Inc., USA), equipped with 90° paddles and a magnetic stir bar, with an agitation of 40 rpm. After the coating process, microcarriers were washed once with StemPro culture medium. 50x10⁶ MSC(M), previously expanded under static conditions with StemPro culture medium for 2 passages, were mixed with the pre-coated plastic microcarriers and the microcarrier-cell suspension (100 mL) was transferred to a 2 L STR (F0 BABY Bioreactor; Bionet, Spain), equipped with a three-blade pitched impeller, and dissolved oxygen (DO), pH, and temperature probes, already containing 500 mL of StemPro culture medium. For process monitoring and control, the F0 BABY was coupled to ROSITA software (Bionet). Process parameters were set to pH 7.2, temperature at 37°C and DO of 20% of air saturation (Dos Santos et al., 2014; Fernandes-Platzgummer et al., 2016). pH control was performed by adding CO₂ through overlay (50 ccm), DO concentration was maintained through overlay (100 ccm) with a mixture of gases (air, CO₂, N₂) and temperature was controlled via thermal jacket. The cell seeding on the microcarriers (first 24 h) was performed under continuous stirring at 40 rpm and afterwards the agitation was increased to 60 rpm. STR cultures were operated under FB and FB/CP mode. For FB cultures, after 3 days with 600 mL of volume, fresh culture medium was added at days 3, 6 and 7 (final volume of 1750 mL). For the FB/CP cultures, from day 3 to day 5.5, 700 mL of fresh culture medium was added at a constant rate of 0.2 mL/min and after reaching a volume of 1300 mL, the STR started to operate under continuous perfusion at the same flow rate (0.22 day⁻¹ dilution rate) until day 11. Cell-containing microcarriers were maintained inside the reactor, by using a Spin Filter mounted in the agitation shaft. To maintain glucose concentration between 2-6 mM, pulses of concentrated glucose (100 g/L, Sigma) were added to the STR daily (days 3-8) or every 2 days (days 4-12) for FB and FB/CP cultures, respectively. At days 9 and 13, the conditioned medium (MSC-CM) from the STR cultures operated under FB and FB/CP, respectively, was separated from the cell-containing microcarriers, streamed through a 0.22 µm filter and stored at -80°C for EVs processing and characterization.

2.4 Monitoring of cell culture in the STR

Cell Counts and Viability

STR culture sampling was performed using a previously established protocol (Fernandes-Platzgummer et al., 2014). Briefly, every day, duplicate samples of evenly mixed culture were collected from the STR and transferred to 2 mL tubes. After the microcarriers settle, the supernatant was collected for glucose/lactate analysis and the cell-containing beads were washed with PBS and incubated with TrypLE solution for 7 min in the thermomixer (Eppendorf AG, Germany) at 37°C and 750 rpm. Afterwards, cells were separated from the microcarriers with a 100 µm cell strainer and the cell number and viability were assessed by using the Trypan Blue exclusion method.

Growth Rate and Doubling Time Calculation

The growth kinetics of MSC(M) cultured under stirred conditions on microcarriers was also characterized. For the exponential phase (considering the death rate constant negligible), the maximum specific growth rate, μ_{\max} (day⁻¹), was calculated as $dX_v/dt = \mu_{\max} \times X_v$, where X_v is the viable cell number for a given time (t). After calculating μ_{\max} , the doubling time, t_d (day), was calculated as $t_d = \ln(2)/\mu_{\max}$.

Glucose/Lactate Analysis

Glucose and lactate concentrations in the samples retrieved from the STR cultures were determined by membrane-bound immobilized enzyme quantification in a YSI 2500 Biochemistry Analyzer (YSI, USA)

DAPI staining (Nuclear integrity)

Every 2 days, samples of cell-containing microcarriers were stained with DAPI (1 mg/mL) (4',6-diamidino-2-phenylindole dihydrochloride, Sigma) for 5 min at room temperature (RT) and protected from light, to observe cell adhesion and distribution on the microcarriers.

Immunophenotypic analysis

MSC(M) were analysed by flow cytometry before and after expansion under stirred conditions, using a panel of mouse anti-human monoclonal antibodies for the expression of CD90 (PE-conjugated), CD73 (phycoerythrin (PE)-conjugated), CD14 (PE-conjugated), CD19 [PE-conjugated], CD34 [fluorescein isothiocyanate (FITC)-conjugated], CD45 (FITC-conjugated) and HLA-DR (PE-conjugated) (all from Biolegend, USA); anti-CD105 (PE-conjugated, InvitrogenTM, Thermo Fisher Scientific, USA) was also used. Briefly, cells were incubated with each antibody for 20 min in the dark and at RT, washed with PBS and then fixed using a solution of 1% (v/v) PFA in PBS. Samples were analysed in a FACScalibur (Becton Dickinson, USA) flow cytometer and CellQuestTM software (Becton Dickinson) was used for acquisition. A minimum of 10 000 events were collected for each sample. Analysis was performed using the FlowJo software (Tree Star, USA).

2.5 MSC-EVs separation by precipitation

MSC-EVs were isolated from the MSC-CM (thawed on ice) using the Total Exosome Isolation Kit (InvitrogenTM) according to manufacturer's instructions (de Almeida Fuzeta et al., 2020). Briefly, 50 ml of MSC-CM were incubated with half the volume of Total Exosome Isolation reagent overnight at 4°C. Afterwards, samples were centrifuged for 1h at 10,000 × *g* and 4°C, the supernatant was removed, and the MSC-EV enriched pellet was resuspended in 1 ml of cold RNase-Free PBS (InvitrogenTM) diluted in UltraPureTM DNase/RNase-free Distilled Water (InvitrogenTM). MSC-EV were aliquoted and stored at -80°C in Eppendorf Protein Lowbind Tubes (Eppendorf AG) until further use.

2.6 MSC-EV characterization

Nanoparticle Tracking Analysis (NTA)

NTA was performed using NanoSight LM14C instrument equipped with a 405 nm laser (Malvern Panalytical, United Kingdom) and the software NanoSight 3.1 (Malvern Panalytical, United Kingdom). Silica 100 nm microspheres (Polysciences, Inc.) were routinely analysed to check instrument performance (Gardiner et al., 2013) and NTA acquisition and post-acquisition settings were optimized and kept constants for all samples. Particle concentration and size distribution on MSC-EVs diluted samples (1:50) were determined according to protocols optimized at iBB described elsewhere (de Almeida Fuzeta et al., 2020).

Protein Quantification

Protein concentration on MSC-EVs samples was measured using Micro BCATM Protein Assay Kit (Thermo ScientificTM) following manufacturer's guidelines. Briefly, bovine serum albumin (BSA) standards and samples were diluted 1:2 with an equal volume of reagent solution and incubated for 2 h at 37°C. Absorbance was measured at 562 nm using the plate reader (BioTek Synergy NEO, software Gen5 version 2.09). Three replicates were quantified for each sample. A linear fit was applied to the BSA standards, and the resulting equation was used to determine each sample concentration from its absorbance measurement.

Purity Assessment

The purity of the MSC-EV samples was given by the particle to protein ratio (PPR), which is the ratio between the particle concentration determined by NTA and the protein concentration measured by MicroBCA protein quantification.

Western Blot

The detection of Calnexin, Synthenin, CD63, CD81 and GAPDH through Western Blot was performed according to the protocol optimized at SCERG and described elsewhere (de Almeida Fuzeta et al., 2020). Primary antibodies included anti-Calnexin (1:1000, BD, USA), anti-Synthenin (1:1000, Abcam, UK), anti-CD63 (1:1000, Genetex, USA), anti-CD81 (1:500, Abcam, UK) and anti-GAPDH (1:1000, Santa Cruz Biotechnology, USA). Secondary antibodies included Goat anti-Mouse IgG (H + L) Cross-Adsorbed Secondary Antibody, HRP (1:5000, InvitrogenTM) and Goat anti-Rabbit IgG HRP-conjugated (1:1000, R&D Systems, UK). Image acquisition was performed on iBrightTM CL1500 Imaging System (InvitrogenTM).

Transmission Electron Microscopy (TEM)

TEM Imaging was performed following negative staining protocol. Briefly, 100 Mesh copper grids were coated with formvar/carbon and glow discharged right before use. MSC-EV samples were mixed (1:1) with formaldehyde 4% in 0.1 M PBS (final concentration 2% formaldehyde in 0.05 M PBS) and incubated for 5 min at RT. Then samples added to the grids and were incubated for 5 min to promote adhesion of EVs to the grids. Next, washing in 10 drops of distilled water was performed and samples were stained in 2 drops of uranyl acetate 2% by incubation for 5 min at RT in the dark followed by sample imaging. A TecnaiTM G² Spirit BioTWIN Transmission Electron Microscope (TECNAI Tecnogroup, Italy) operating at 120k was used, and data was collected with an Olympus-SIS Veleta CCD Camera (OLYMPUS, Japan).

2.7 Statistical Analysis

Results are presented as mean \pm standard error of the mean (SEM) of the values obtained from different MSC donors (i.e., biological replicates). When appropriate, comparisons between experimental results were determined by the non-parametric Mann–Whitney U test and statistical significance was assessed with a p-value less than 0.05.

RESULTS

3.1 Influence of the feeding strategy on MSC(M) proliferation

Based on previous work from our group (Dos Santos et al., 2014), a S/X-free microcarrier-based culture system was successfully established for MSC(M) proliferation using a 2 L-scale fully controlled STR operated under FB and FB/CP modes. 50×10^6 MSC(M) from 3 donors were expanded on CellStart-coated plastic microcarriers with S/X-free StemPro culture medium, which varied over culture time as shown in Figure 1A. During the adhesion stage (first 24 h of cultivation), a minimum agitation speed of 40 rpm was used, which simultaneously allowed to keep the microcarriers in suspension, maximizing the cell-microcarrier contact necessary for cell adhesion, and minimized cell death due to agitation (Hewitt et al., 2011). Subsequently, the agitation speed was increased to 60 rpm to avoid/minimize the formation of aggregates. After 24 hours, cell adhesion efficiencies of $(34 \pm 5.8)\%$ and $(40 \pm 5.9)\%$ corresponding to $(1.9 \pm 0.19) \times 10^7$ and $(2.1 \pm 0.23) \times 10^7$ cells were attained for FB and FB/CP, respectively. Throughout the STR experiments, for both feeding operation modes, cell viabilities were always above 90%, and the fraction of live/dead cells found in suspension was $(5.8 \pm 1.3)\%$, after day 2. The growth curves depicted in Figure1B display an exponential phase leading to maximal cell numbers of $(3.0 \pm 0.12) \times 10^8$ and $(5.3 \pm 0.32) \times 10^8$ corresponding to cell densities of $(2.0 \pm 0.51) \times 10^5$ and $(4.1 \pm 0.90) \times 10^5$ cells/mL (Figure1B) and fold increase (FI) values in total cell number of 16 ± 2.1 and 24 ± 5.5 (Figure1C), obtained at days 8 and 12 of cultivation for FB and FB/CP cultures, respectively. No major differences were observed in terms of cell number until day 7 for the two feeding operation modes tested. After this day, cell growth ceased in the STR operating under FB mode. Specific growth rates (μ_{\max}) and doubling times (t_d) were also calculated for the two STR feeding operation modes according to “Materials and Methods” and were $0.6 \pm 0.1 \text{ day}^{-1}$ and $1.3 \pm 0.2 \text{ days}$; and $0.5 \pm 0.1 \text{ day}^{-1}$ and $1.5 \pm 0.2 \text{ days}$, respectively, for FB and FB/CP cultures.

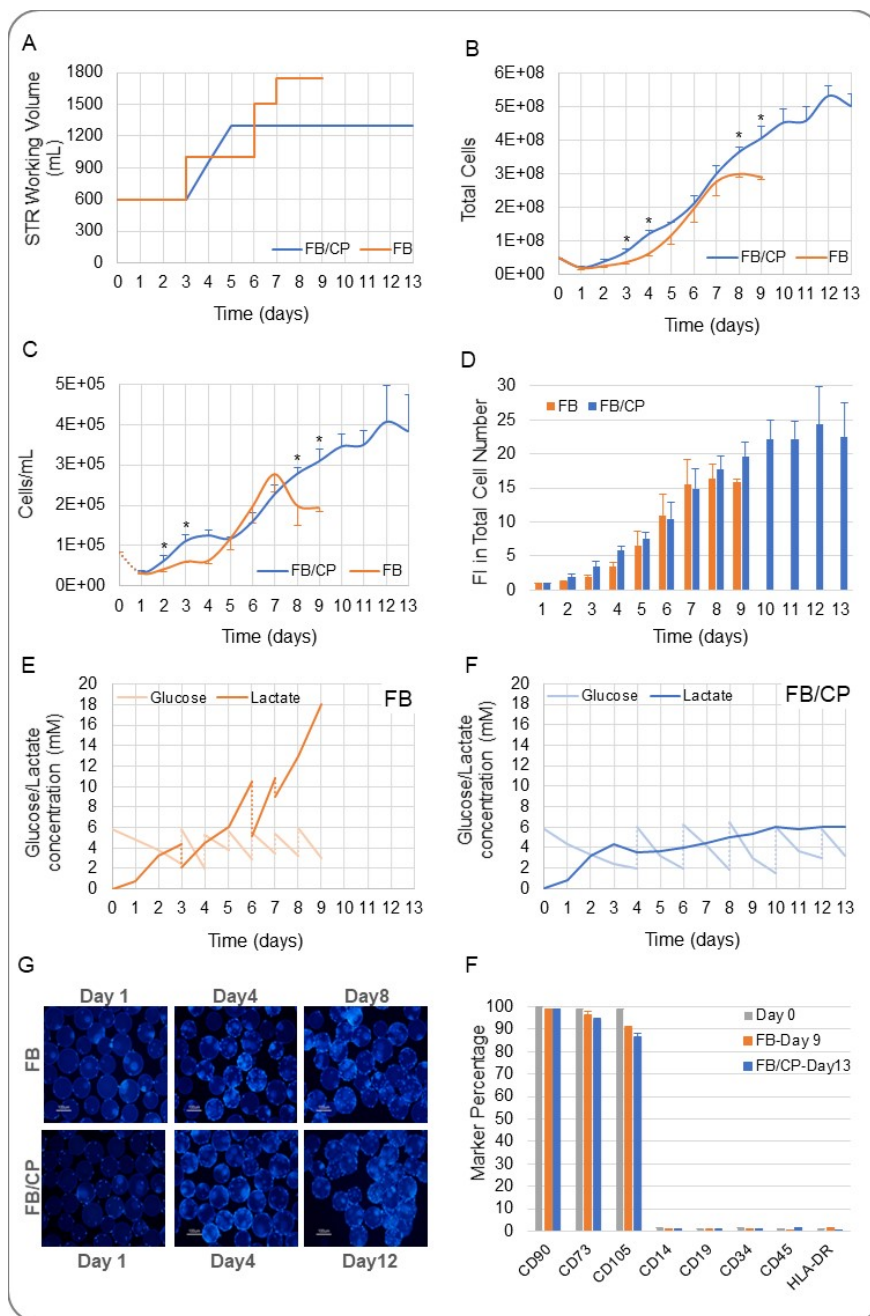


Figure 1: *Ex-vivo* expansion of human bone marrow-derived mesenchymal stromal cells MSC(M) in a fully controlled stirred tank reactor (STR) operated under fed-batch (FB) or FB combined with continuous perfusion (FB/CP) operation mode. (A) STR working volume during FB (orange line) and FB/CP (blue line) cultures. Growth curves in terms of total cell number (B) and cells per mL (C) of MSC(M) expanded on microcarriers in the STR operated under FB (orange line) or FB/CP (blue line) operation mode (* $P \leq 0.05$). (D) Fold increase (FI) value in total cell number estimated per day during FB (orange bars) and FB/CP (blue bars) cultures. FI is the ratio between the number of cells counted each day and the number of cells that adhered at day 1. Glucose (light colour line) and lactate (dark colour line) concentrations attained during time in culture for FB (E) and FB/CP (F) cultures. (G) Representative images of microcarrier occupancy for FB and FB/CP at Day 1, Day 4, and Day 8/12.

by MSC(M) stained with DAPI throughout STR cultures. (F) Immunophenotypic analysis before (light grey bars) and after expansion in the STR under FB (orange bars) or FB/CP (blue bars) operation modes. 50×10^6 MSC(M) from 3 donors were expanded on CellStart-coated plastic microcarriers with xenogeneic/serum-free (X/S-free) StemPro culture medium. For FB cultures, after 3 days with 600 mL of volume, fresh culture medium was added at days 3, 6 and 7. For FB/CP cultures, from day 3 to day 5.5, 700 mL of fresh culture medium was added at a constant rate of 0.2 mL/min and after reaching a volume of 1300 mL, the STR started to operate under continuous perfusion at the same flow rate (0.22 day^{-1} dilution rate) until day 11. Cell-containing microcarriers were maintained inside the bioreactor, by using a Spin Filter mounted in the agitation shaft. To maintain glucose concentration between 2-6 mM, pulses of concentrated glucose were added to the STR daily (days 3-8) or every 2 days (days 4-12) for FB and FB/CP cultures, respectively. Results are presented as mean \pm standard error of the mean ($n=3$). STR: stirred tank reactor, FB: fed-batch, FB/CP: fed-batch combined with continuous medium perfusion.

In what concerns metabolic activity, the glucose and lactate concentration profiles over time (Figure 1E and F) show that the adopted feeding schemes maintained glucose levels within the target range (2-6 mM), whereas lactate concentration, as expected, increases until reaching a maximum of 18 mM at day 9 in FB cultures and remains relatively constant below 6 mM in FB/CP cultures. To evaluate qualitatively cell adhesion and proliferation of MSC immobilized on the microcarriers during time in culture, DAPI staining was performed every 2 days for the different culture conditions tested (FB and FB/CP operation modes). For both conditions, after the first 24h, a homogenous cell distribution on the microcarriers was observed, followed by a gradual increase in microcarrier occupancy by MSC throughout time in the culture. At the end of culture, some cell-containing microcarrier aggregation was observed, mainly for FB/CP cultures (Day 12) (Figure 1G). At the end of STR cultures, cells were detached from the microcarriers and characterized by immunophenotypic analysis (Figure 1H). MSC(M) demonstrated high levels ($>94\%$) of CD90 and CD73 and low expression ($<3\%$) of CD14, CD19, CD34, CD45 and HLA-DR antigens before and after cell expansion in STR operated under both feeding operation modes, with no major differences between them. Concerning CD105, a decrease in its expression was observed after cell expansion under stirred conditions [($99 \pm 0.51\%$)% at day 0 to ($90 \pm 0.59\%$)% and ($87 \pm 1.5\%$)% at day 8 and day 12, for FB and FB/CP, respectively] (Figure 1H).

3.2 Production of MSC-EVs in STR operated under FB or FB/CP operation mode

In the final two days of culture, for both FB and FB/CP cultures (day 7 and 11, respectively), no fresh culture medium was added, nor exhausted medium removed from the STR, to concentrate the production of EVs. Only concentrated glucose pulses were provided at days 8 and 12 for FB and FB/CP cultures, respectively, to avoid glucose exhaustion. After EV conditioning phase (last 2 days), the conditioned medium (MSC-CM) was collected, and the EVs were successfully isolated and characterized according to “Materials and Methods” section. EVs isolated from the MSC-CM of all STR cultures were identified by TEM and Western blot. Representative TEM images depicted in Figure 2A, show individual vesicles presenting a “cup-shaped morphology” due to the adsorption of the EVs onto the hard surface and drying.

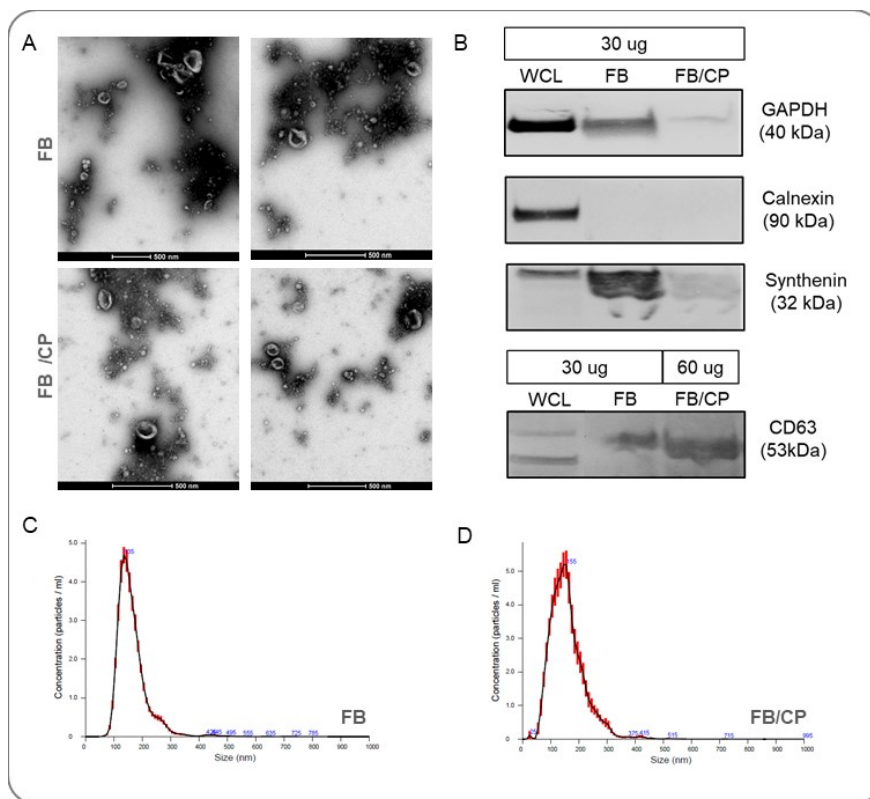


Figure 2: Characterization of human MSC-derived extracellular vesicles MSC-EVs produced in a fully-controlled STR operated under FB or FB/CP operation mode. 50×10^6 MSC(M) from 3 donors were expanded on CellStart-coated plastic microcarriers with S/X-free StemPro culture medium. In the end of the EVs conditioning phase (last 2 days), at days 9 and 13, the MSC-CM from FB and FB/CP cultures, respectively, were separated from the cell-containing microcarriers, streamed through a $0.22 \mu\text{m}$ filter and stored at -80°C for EVs isolation and characterization. (A) Representative TEM images of MSC-EVs from STR cultures. (B) Representative western blot images of MSC lysates and MSC-EVs samples. Detection of the housekeeping protein GAPDH, calnexin, synthenin and CD63 in MSC-EVs and corresponding WCL (i.e., cells) obtained from the STR operated under FB and FB/CP. Representative size distribution curves of EVs samples iso-

lated from MSC-CM from FB (C) and FB/CP (D) cultures. WCL: whole cell lysates, STR: stirred tank reactor, FB: fed-batch, FB/CP: fed-batch combined with continuous medium perfusion, TEM: transmission electron microscopy.

The presence of EVs was also confirmed by Western blot analysis (Figure 2B). The EV protein markers synthenin and CD63 were successfully detected in EV samples, while calnexin, an endoplasmic reticulum protein, was present in cells but absent in EV samples, as expected. The size distribution of MSC-EVs was determined by NTA. In Figure 2C and D are depicted two representative size distribution curves for EVs isolated from MSC-CM from FB and FB/CP STR cultures, respectively. Isolated EVs showed an equivalent size distribution profile enriched in small EVs (<200nm) (Figure 2C and D). EVs mean and mode sizes were respectively (163±5.27) nm and (134±4.23) nm for FB cultures and (162±4.44) nm and (137±6.92) nm for FB/CP cultures Table 1(p>0.05). Moreover, the concentration of EVs in the MSC-CM from the STR cultures was also estimated by NTA. As presented in Table 1, average concentrations of (2.4±0.35)×10¹¹ and (3.0±0.48)×10¹¹ EVs/ml corresponding to (4.2±0.61)×10¹⁴ and (3.9±0.62)×10¹⁴EVs were estimated for EVs isolated from MSC-CM from STR operated under FB and FB/CP, respectively.

Table 1: MSC-EVs characteristics and concentration in MSC-CM.

	EVs Mean size (nm)	EVs Mode size (nm)	Protein concentration (mg/ml)	EV concentration (
FB	163±5.27	134±4.23	1.4±0.16	2.4±0.35
FB/CP	162±4.44	137±6.92	1.5±0.10	3.0±0.48

50×10⁶ MSC(M) from 3 donors were expanded on CellStart-coated plastic microcarriers with S/X-free StemPro culture medium. In the end of the EVs conditioning phase (last 2 days), at days 9 and 13, the MSC-CM from FB and FB/CP cultures, respectively, were separated from the cell-containing microcarriers, streamed through a 0.22 µm filter and stored at -80°C for EVs isolation and characterization. Results are presented as mean ± SEM. MSC-EV: mesenchymal stromal cell-derived extracellular vesicles, MSC-CM: mesenchymal stromal cell-derived conditioned medium, PPR: particle to protein ratio, FB: fed-batch, FB combined with continuous perfusion: FB/CP, STR: stirred tank reactor

Although the total number of EVs in the FB/CP-derived MSC-CM is lower, when compared with FB-derived MSC-CM, this value is underestimated, since, due to continuous operation the EVs did not accumulate in the reactor, as happened in the cultures operated under FB mode. To assess the purity of EV samples, particle to protein ratio (PPR) was also determined by dividing the EV concentration estimated by NTA, by the total protein concentration determined with BCA protein assay. High PPR means high sample purity due to low amount of co-isolated protein contaminants. As presented in Table 1 , EV samples isolated from MSC-CM from STR cultures operated under FB and FB/CP, presented similar PPRs of (1.7±0.21) ×10⁸ and (2.0±0.22) ×10⁸ particle/µg protein, respectively. Table 2 summarizes all parameters of the MSC(M) expansion process and the production of its EVs in STR operated under FB or FB/CP mode.

Table 2: Comparison of different process parameters of the expansion of MSC(M) and production of MSC-EVs in STR cultures operated under FB and FB/CP modes.

MSC(M)

MSC-EV

50×10^6 MSC(M) from 3 donors were expanded on CellStart-coated plastic microcarriers with S/X-free StemPro culture me

DISCUSSION

Over the last years, numerous basic and clinical studies have focused on MSC due to their powerful regenerative potential and immunomodulatory features [reviewed in (Zhou et al., 2021)]. More recently, most of the potential beneficial effects of MSC therapies have been primarily attributed to EVs, with several studies confirming that EVs recapitulate many of the features of their parental cell line (MSC). Overall, MSC-EVs have been being explored for the potential treatment of spinal cord injury (Wang et al., 2021), acute kidney injury (Bruno et al., 2012), atherosclerotic cardiovascular disease (Badimon et al., 2022), myocardial ischemia (Charles et al., 2020; Ma et al., 2017; Zhu et al., 2018), among other diseases. To support all these clinical applications, large doses of EVs will be required and the limited manufacture capacity of traditional static culture systems will be a major hurdle towards the implementation of EVs-based therapies. In this context, the large-scale production of therapeutic MSC and their EVs will require the development of a cost-effective manufacturing platform based on fully controlled bioreactor systems for the expansion of well-characterized MSC populations and the production of their MSC-CM, as well as a robust downstream process to isolate and purify MSC and MSC-EVs [reviewed in (Mawji et al., 2022; Syromiatnikova et al., 2022)]. In this work, a S/X-free microcarrier-based culture system was successfully established for the expansion of MSC(M) and the production of MSC-EV using a 2 L-scale controlled STR as it represents a scalable, robust, cost-effective, and well-characterized platform widely used to produce biotherapeutics. In our previous work, MSC(M) and umbilical cord-derived Wharton’s jelly MSC [MSC(WJ)] were expanded on CellStart-coated plastic and Cultispher *S* microcarriers, respectively, using S/X-free StemPro culture medium and a bench-scale STR (1L) operated under repeated medium exchange mode (Dos Santos et al., 2014; Fernandes-Platzgummer et al., 2016). Based on those works, the operational process parameters were set to pH 7.2, dissolved oxygen (DO) 20%, temperature 37°C and agitation rate 60 rpm (40 rpm during cell adhesion to the microcarriers). The entire culture was carried out in the STR, representing an advance compared to our previous protocol, where cell adhesion and initial culture (4 days) were performed in a spinner flask and subsequently transferred to the reactor (i.e. cell-containing microcarriers plus culture medium) (Dos Santos et al., 2014). After 24h, MSC(M) successfully adhered to the microcarriers, with adhesion efficiencies between 30-50%, and with a very homogeneous cell distribution, a factor identified to be crucial for a successful microcarrier-based culture (Carmelo et al., 2015). Despite losing more than 50% of the inoculated cells, carrying out the entire process inside the reactor has the advantages of having the whole protocol controlled from the first day of culture, while minimizing the risk of contamination associated to transferring the cell suspension between culture systems. Additionally, the adhesion efficiency can be maximized by optimizing the culture conditions in the first 24h, including the use of other agitation regimes or alternative microcarriers [reviewed in (Tsai & Pacak, 2021)]. For example, in previous studies from our group under S/X-free culture conditions, adhesion efficiencies of MSC(WJ) on gelatin-based *Cultispher S* microcarriers around 75% were attained in a 2L bioreactor culture (Mizukami et al., 2016), whereas initial adhesion efficiencies of 71 ± 7.4 and $74 \pm 0.3\%$ were obtained for MSC(M) using Low Concentration SynthemaxTM II and CellBIND® microcarriers, respectively, in spinner flask cultures (Carmelo et al., 2015).

Since culture medium represents one of the major costs in the manufacturing of human MSC, the delineation of feeding strategies able to maximize cell densities in a cost-effective way is of utmost importance. The feeding scheme adopted in most dynamic microcarrier-based culture systems used to expand MSC, is the repeated medium exchange strategy, where the cell-containing beads are allowed to settle before changing

the culture medium once or twice a day (Cunha et al., 2015; de Almeida Fuzeta et al., 2020; Dos Santos et al., 2014; Lembong et al., 2020). This procedure requires stopping the reactor operation (i.e. discontinuous operation), which has the disadvantage of increasing the probability of aggregation between the cell-containing microcarriers during stagnant periods, potentially impairing cell growth and impacting cell identity. In this work, we hypothesized that an automated feeding protocol would potentially result in fewer fluctuations in cell proliferation/metabolism patterns and that a continuous operation would minimize cell-containing microcarrier aggregation. Therefore, two feeding operation modes were compared: FB, where the fresh culture medium was added discretely to the STR and FB/CP, where there was an automated continuous removal/replenishment of the medium with retention of the cell-containing microcarriers through a spin-filter. Growth curves of MSC(M) expanded under the two feeding regime strategies were quite similar during the first 6-7 days of cultivation, diverging upon this time point to reach considerable different maximal cell densities of $(2.0 \pm 0.51) \times 10^5$ and $(4.1 \pm 0.90) \times 10^5$ cells/mL at days 8 and 12 of cultivation for FB and FB/CP cultures, respectively. This difference could be explained by the accumulation of toxic by-products such as lactate, although it never reached values described as inhibitory to cell growth (35 mM (Schop et al., 2009)), and/or by the lack of replenishment of other important nutrients, as glucose concentration in the culture medium was always ranging from 2-6 mM, above the non-limiting value (over 1 mM (Schop et al., 2009)). Indeed, the concentrated glucose pulses added throughout culture, allowed us to maintain the glucose concentration within the desire range without adding volumetric capacity to the bioreactor.

Overall, continuous medium perfusion operation allowed MSC expanded under S/X-free conditions to reach densities in the STR that had previously only been achieved on small scale stirred culture systems ([?]400 mL) operated under S/X-free conditions (Cunha et al., 2015), or often employing culture media containing human serum components (de Almeida Fuzeta et al., 2020; Lembong et al., 2020). The specific growth rates estimated were 0.6 ± 0.1 and 0.5 ± 0.1 for FB and FB/CP cultures, respectively, which are in agreement with the literature for MSC cultures cultured under S/X-free conditions (Carmelo et al., 2015; Cunha et al., 2015; Heathman et al., 2018). Other studies have compared different feeding modes of operation. In a previous work by our group, two different feeding regimes were compared for MSC(M) cultivation using a combined system employing a spinner flask transferred thereafter to a 1L-scale controlled STR: daily medium renewal every day or every 2 days *versus* fed-batch addition of concentrated nutrients and growth factors every 2 days. No significant differences were observed in terms of MSC(M) proliferation, although the fed-batch approach led to a faster accumulation of metabolites, namely lactate, as expected, as no culture medium was withdrawn from the STR. Moreover, a continuous perfusion process was tested in a smaller 400 mL STR with a dilution rate of 0.25 day^{-1} (starting from day 3) throughout the whole process. A maximal cell density of 5.0×10^5 cells/mL was reached at day 11, demonstrating the advantage of working under perfusion operation mode (Dos Santos et al., 2014). Cunha and colleagues also compared two different culture operation modes for expanding MSC(M) in a STR, 50% medium renewal every 2.5 days *versus* continuous perfusion cultures at a dilution rate of 0.2 day^{-1} . The results attained showed that MSC achieved higher cell concentrations (3.7×10^5 cell/mL) and maximum growth rate (0.38 day^{-1}) in continuous perfusion cultures when compared to the repeated medium exchange strategy (2.9×10^5 cell/mL and 0.26 day^{-1}), respectively. Although continuous perfusion processes led to higher cell densities when compared to fed-batch or repeated medium exchange operation modes, it utilizes larger quantities of culture media, which increases the operation costs. Moreover, the greater logistic of implementing it (especially in what concerns the cell retention device) and higher probability of technical failures have been hindering the use of this feeding operation mode for the production of MSC. In the present work, a spin-filter was used to retain the cell-containing microcarriers inside the STR. This system consists in a cylinder cage with a porous mesh wall, normally mounted on the impeller shaft. Perfusate (bleed) is pumped out from inside the spin-filter at the same rate at which fresh culture medium is pumped into the bulk of the STR (i.e. outside the spin-filter). Minimum fouling and an optimum cell retention at the necessary medium perfusion rate are crucial parameters for a successful operation of a spin-filter-based STR (Castilho & Medronho, 2002). No fouling phenomenon was observed in the mesh of the spin-filter in the present work and the cell-containing microcarriers were efficiently retained inside the STR, as no microcarriers were detected in the STR bleed. Another important parameter in continuous perfusion cultures is the dilution rate, as low perfusion rates result in growth inhibition due to nutrient exhaustion

and/or accumulation of metabolites, and high perfusion rates results in wasting valuable medium components and over dilution of autocrine factors promoters of cell growth. In this context, as it has been previously demonstrated for human hematopoietic stem/progenitor cells (Madlambayan et al., 2005), the expansion of stem cell populations can be boosted by removing inhibitory factors produced by their more differentiated progeny. For those reasons, it would be interesting in the future to study different medium residences times in the STR platform operating under a continuous perfusion mode and their impact on MSC attributes.

Immunophenotype analysis before and after STR cultures revealed that MSC(M) cultured in S/X-free culture medium under stirred conditions maintained the high expression of CD73, CD90, and CD105, whereas the expression levels of hematopoietic cell markers (CD34, CD45, CD14 and CD19), and HLA-DR molecules were very low in all conditions, satisfying the minimal phenotypic criteria for describing human MSC (Viswanathan et al., 2019). The expression of CD105 decreased after the STR cultures, which was expected, as this event has been reported previously by our group and others (de Soure et al., 2016; Dos Santos et al., 2014), and may be attributed to longer exposure times to the enzymatic agent for cell detachment, which is known to affect surface receptors (Brown et al., 2007; Tsuji et al., 2017).

Overall, the results obtained in this work are in line with previous results from our group and others showing that MSC main features are well maintained upon cultivation under S/X-free stirred conditions (Carmelo et al., 2015; Cunha et al., 2015; Dos Santos et al., 2014).

At the end of STR cultures, the MSC-CM was collected and the EVs were successfully isolated and characterized by different techniques proposed by the International Society of Extracellular Vesicles (Witwer et al., 2017). TEM and Western blot techniques confirm the “cup-shaped” morphology of EVs and the presence of their characteristic markers, respectively and no significant different were found between EVs mean and mode sizes [(163+-5.27) nm *vs* (162+-4.44) nm and (134+-4.23) nm *vs* (137+-6.92) nm] for FB and FB/CP cultures, respectively ($P>0.05$). In what concerns the concentration of EVs and their purity in the MSC-CM retrieved from the STR cultures, average concentrations of $(2.4\pm 0.35)\times 10^{11}$ and $(3.0\pm 0.48)\times 10^{11}$ EVs/ml and similar PPRs of $(1.7\pm 0.21)\times 10^8$ and $(2.0\pm 0.22)\times 10^8$ particle/ μ g protein were estimated by NTA and protein quantification for FB and FB/CP cultures, respectively. The MSC-EV densities obtained herein and in agreement with the results reported on the production of MSC-EVs using microcarriers in a Vertical-Wheel bioreactor (VWBR) by our group (de Almeida Fuzeta et al., 2020) in spinner flasks by others (Haraszti et al., 2018). To the best of our knowledge, this is the first work describing a fully controlled process that maximizes the proliferation of MSC(M) under S/X-free conditions in a 2L STR and the subsequent isolation of EVs from the enriched MSC-derived conditioned medium.

Conclusions

The bioreactor-based platform developed herein will allow to transform laboratory-based protocols into robust MSC and MSC-EVs manufacturing processes, with a tight control over the culture process and significant reduction of the production times. By addressing the manufacturing challenges of cell-based products, this technology is expected to facilitate translation of MSC therapies and likely to impact the development of therapeutic strategies employing MSC-EVs, which could rapidly progress towards clinical studies exploiting their potential as intrinsic therapeutics or as drug delivery systems (de Almeida Fuzeta et al., 2022; Syromiatnikova et al., 2022). In addition, this platform could be applied to the production of EVs from other parental cells lines (i.e. dendritic cells, natural killer cells) in therapeutic settings as cancer.

Author Contributions : Ana Fernandes-Platzgummer: Conceptualization, Investigation, Methodology, Writing - Original Draft, Funding Acquisition. Raquel Cunha: Investigation, Methodology; Marta Carvalho: Investigation; Sara Morini: Investigation; Juan Moreno-Cid: Methodology; Joaquim M.S. Cabral: Funding acquisition and Writing - Review & Editing; Cláudia Lobato da Silva: Conceptualization, Writing - Review & Editing and Funding Acquisition. All authors have read and agreed to the published version of the manuscript.

Acknowledgments : We would like to acknowledge Instituto Português de Oncologia Francisco Gentil and

Clínica de Todos-os-Santos for their kind donations of BM samples for this study.

Funding : This research was financed by national funds from FCT—Fundação para a Ciência e Tecnologia (FCT), I.P., within the scope of the projects UIDB/04565/2020 and UIDP/04565/2020 of the Research Unit Institute for Bioengineering and Biosciences-iBB, LA/P/0140/2020 of the Associate Laboratory Institute for Health and Bioeconomy—i4HB, and PTDC/EQU-EQU/31651/2017 of the EXOpro project. This research was also funded by the project Bioprocessing Strategies for high productivity in the Culture of Human Stem Cells in Stirred Tank Bioreactors and their downstream. CELLS4ALL H2020-INNOVOUCHER-2018-0039.

Conflicts of Interest : J.M.-C. is employee of Bionet company.

REFERENCES

- Alvarez-Erviti, L., Seow, Y., Yin, H., Betts, C., Lakhali, S., & Wood, M. J. (2011). Delivery of siRNA to the mouse brain by systemic injection of targeted exosomes. *Nat Biotechnol* , 29 (4), 341-345. <https://doi.org/10.1038/nbt.1807>
- Badimon, L., Padro, T., Arderiu, G., Vilahur, G., Borrell-Pages, M., & Suades, R. (2022). Extracellular vesicles in atherothrombosis: From biomarkers and precision medicine to therapeutic targets. *Immunol Rev* , 312 (1), 6-19. <https://doi.org/10.1111/imr.13127>
- Baglio, S. R., Rooijers, K., Koppers-Lalic, D., Verweij, F. J., Perez Lanzon, M., Zini, N., . . . Pegtel, D. M. (2015). Human bone marrow- and adipose-mesenchymal stem cells secrete exosomes enriched in distinctive miRNA and tRNA species. *Stem Cell Res Ther* , 6 (1), 127. <https://doi.org/10.1186/s13287-015-0116-z>
- Balbi, C., Piccoli, M., Barile, L., Papait, A., Armirotti, A., Principi, E., . . . Bollini, S. (2017). First Characterization of Human Amniotic Fluid Stem Cell Extracellular Vesicles as a Powerful Paracrine Tool Endowed with Regenerative Potential. *Stem Cells Transl Med* , 6 (5), 1340-1355. <https://doi.org/10.1002/sctm.16-0297>
- Brown, M. A., Wallace, C. S., Anamelechi, C. C., Clermont, E., Reichert, W. M., & Truskey, G. A. (2007). The use of mild trypsinization conditions in the detachment of endothelial cells to promote subsequent endothelialization on synthetic surfaces. *Biomaterials* , 28 (27), 3928-3935. <https://doi.org/10.1016/j.biomaterials.2007.05.009>
- Bruno, S., Grange, C., Collino, F., Deregibus, M. C., Cantaluppi, V., Biancone, L., . . . Camussi, G. (2012). Microvesicles derived from mesenchymal stem cells enhance survival in a lethal model of acute kidney injury. *PLoS One* , 7 (3), e33115. <https://doi.org/10.1371/journal.pone.0033115>
- Camussi, G., Deregibus, M. C., & Cantaluppi, V. (2013). Role of stem-cell-derived microvesicles in the paracrine action of stem cells. *Biochem Soc Trans* , 41 (1), 283-287. <https://doi.org/10.1042/BST20120192>
- Carmelo, J. G., Fernandes-Platzgummer, A., Diogo, M. M., da Silva, C. L., & Cabral, J. M. (2015). A xeno-free microcarrier-based stirred culture system for the scalable expansion of human mesenchymal stem/stromal cells isolated from bone marrow and adipose tissue. *Biotechnol J* , 10 (8), 1235-1247. <https://doi.org/10.1002/biot.201400586>
- Castilho, L. R., & Medronho, R. A. (2002). Cell retention devices for suspended-cell perfusion cultures. *Adv Biochem Eng Biotechnol* , 74 , 129-169. https://doi.org/10.1007/3-540-45736-4_7
- Cerri, S., Greco, R., Levandis, G., Ghezzi, C., Mangione, A. S., Fuzzati-Armentero, M. T., . . . Blandini, F. (2015). Intracarotid Infusion of Mesenchymal Stem Cells in an Animal Model of Parkinson's Disease, Focusing on Cell Distribution and Neuroprotective and Behavioral Effects. *Stem Cells Transl Med* , 4 (9), 1073-1085. <https://doi.org/10.5966/sctm.2015-0023>

- Charles, C. J., Li, R. R., Yeung, T., Mazlan, S. M. I., Lai, R. C., de Kleijn, D. P. V., . . . Richards, A. M. (2020). Systemic Mesenchymal Stem Cell-Derived Exosomes Reduce Myocardial Infarct Size: Characterization With MRI in a Porcine Model. *Front Cardiovasc Med* , 7 , 601990. <https://doi.org/10.3389/fcvm.2020.601990>
- Cunha, B., Aguiar, T., Silva, M. M., Silva, R. J., Sousa, M. F., Pineda, E., . . . Alves, P. M. (2015). Exploring continuous and integrated strategies for the up- and downstream processing of human mesenchymal stem cells. *J Biotechnol* , 213 , 97-108. <https://doi.org/10.1016/j.jbiotec.2015.02.023>
- de Almeida Fuzeta, M., Bernardes, N., Oliveira, F. D., Costa, A. C., Fernandes-Platzgummer, A., Farinha, J. P., . . . da Silva, C. L. (2020). Scalable Production of Human Mesenchymal Stromal Cell-Derived Extracellular Vesicles Under Serum-/Xeno-Free Conditions in a Microcarrier-Based Bioreactor Culture System. *Front Cell Dev Biol* , 8 , 553444. <https://doi.org/10.3389/fcell.2020.553444>
- de Almeida Fuzeta, M., Goncalves, P. P., Fernandes-Platzgummer, A., Cabral, J. M. S., Bernardes, N., & da Silva, C. L. (2022). From Promise to Reality: Bioengineering Strategies to Enhance the Therapeutic Potential of Extracellular Vesicles. *Bioengineering (Basel)* , 9 (11). <https://doi.org/10.3390/bioengineering9110675>
- de Soure, A. M., Fernandes-Platzgummer, A., da Silva, C. L., & Cabral, J. M. (2016). Scalable microcarrier-based manufacturing of mesenchymal stem/stromal cells. *J Biotechnol* , 236 , 88-109. <https://doi.org/10.1016/j.jbiotec.2016.08.007>
- Dos Santos, F., Andrade, P. Z., Boura, J. S., Abecasis, M. M., da Silva, C. L., & Cabral, J. M. (2010). Ex vivo expansion of human mesenchymal stem cells: a more effective cell proliferation kinetics and metabolism under hypoxia. *J Cell Physiol* , 223 (1), 27-35. <https://doi.org/10.1002/jcp.21987>
- Dos Santos, F., Campbell, A., Fernandes-Platzgummer, A., Andrade, P. Z., Gimble, J. M., Wen, Y., . . . Cabral, J. M. (2014). A xenogeneic-free bioreactor system for the clinical-scale expansion of human mesenchymal stem/stromal cells. *Biotechnol Bioeng* , 111 (6), 1116-1127. <https://doi.org/10.1002/bit.25187>
- Duijvestein, M., Vos, A. C., Roelofs, H., Wildenberg, M. E., Wendrich, B. B., Verspaget, H. W., . . . Hommes, D. W. (2010). Autologous bone marrow-derived mesenchymal stromal cell treatment for refractory luminal Crohn's disease: results of a phase I study. *Gut* , 59 (12), 1662-1669. <https://doi.org/10.1136/gut.2010.215152>
- Elsharkasy, O. M., Nordin, J. Z., Hagey, D. W., de Jong, O. G., Schiffelers, R. M., Andaloussi, S. E., & Vader, P. (2020). Extracellular vesicles as drug delivery systems: Why and how? *Adv Drug Deliv Rev* , 159 , 332-343. <https://doi.org/10.1016/j.addr.2020.04.004>
- Fan, B., Li, C., Szalad, A., Wang, L., Pan, W., Zhang, R., . . . Liu, X. S. (2020). Mesenchymal stromal cell-derived exosomes ameliorate peripheral neuropathy in a mouse model of diabetes. *Diabetologia* , 63 (2), 431-443. <https://doi.org/10.1007/s00125-019-05043-0>
- Fernandes-Platzgummer, A., Carmelo, J. G., da Silva, C. L., & Cabral, J. M. (2016). Clinical-Grade Manufacturing of Therapeutic Human Mesenchymal Stem/Stromal Cells in Microcarrier-Based Culture Systems. *Methods Mol Biol* , 1416 , 375-388. https://doi.org/10.1007/978-1-4939-3584-0_22
- Fernandes-Platzgummer, A., Lobato da Silva, C., & Cabral, J. (2014). Maximizing mouse embryonic stem cell production in a stirred tank reactor by controlling dissolved oxygen concentration and continuous perfusion operation *Biochemical Engineering Journal* , 82 , 81-90.
- Garcia-Olmo, D., Garcia-Arranz, M., Herreros, D., Pascual, I., Peiro, C., & Rodriguez-Montes, J. A. (2005). A phase I clinical trial of the treatment of Crohn's fistula by adipose mesenchymal stem cell transplantation. *Dis Colon Rectum* , 48 (7), 1416-1423. <https://doi.org/10.1007/s10350-005-0052-6>
- Gardiner, C., Ferreira, Y. J., Dragovic, R. A., Redman, C. W., & Sargent, I. L. (2013). Extracellular vesicle sizing and enumeration by nanoparticle tracking analysis. *J Extracell Vesicles* , 2 . <https://doi.org/10.3402/jev.v2i0.19671>

- Haraszti, R. A., Miller, R., Stoppato, M., Sere, Y. Y., Coles, A., Didiot, M. C., . . . Khvorova, A. (2018). Exosomes Produced from 3D Cultures of MSCs by Tangential Flow Filtration Show Higher Yield and Improved Activity. *Mol Ther* , 26 (12), 2838-2847. <https://doi.org/10.1016/j.ymthe.2018.09.015>
- Heathman, T. R. J., Nienow, A. W., Rafiq, Q. A., Coopman, K., BoKara, & Hewitt, C. J. (2018). Agitation and aeration of stirred-bioreactors for the microcarrier culture of human mesenchymal stem cells and potential implications for large-scale bioprocess development. *Biochemical Engineering Journal* , 136 , 9-17. <https://doi.org/10.1016/j.bej.2018.04.011>
- Hewitt, C. J., Lee, K., Nienow, A. W., Thomas, R. J., Smith, M., & Thomas, C. R. (2011). Expansion of human mesenchymal stem cells on microcarriers. *Biotechnol Lett* , 33 (11), 2325-2335. <https://doi.org/10.1007/s10529-011-0695-4>
- Horwitz, E. M., Gordon, P. L., Koo, W. K., Marx, J. C., Neel, M. D., McNall, R. Y., . . . Hofmann, T. (2002). Isolated allogeneic bone marrow-derived mesenchymal cells engraft and stimulate growth in children with osteogenesis imperfecta: Implications for cell therapy of bone. *Proc Natl Acad Sci U S A* , 99 (13), 8932-8937. <https://doi.org/10.1073/pnas.132252399>
- Horwitz, E. M., Prockop, D. J., Fitzpatrick, L. A., Koo, W. W., Gordon, P. L., Neel, M., . . . Brenner, M. K. (1999). Transplantability and therapeutic effects of bone marrow-derived mesenchymal cells in children with osteogenesis imperfecta. *Nat Med* , 5 (3), 309-313. <https://doi.org/10.1038/6529>
- Hyland, M., Mennan, C., Wilson, E., Clayton, A., & Kehoe, O. (2020). Pro-Inflammatory Priming of Umbilical Cord Mesenchymal Stromal Cells Alters the Protein Cargo of Their Extracellular Vesicles. *Cells* , 9 (3). <https://doi.org/10.3390/cells9030726>
- Katsuda, T., Kosaka, N., Takeshita, F., & Ochiya, T. (2013). The therapeutic potential of mesenchymal stem cell-derived extracellular vesicles. *Proteomics* , 13 (10-11), 1637-1653. <https://doi.org/10.1002/pmic.201200373>
- Kay, A. G., Treadwell, K., Roach, P., Morgan, R., Lodge, R., Hyland, M., . . . Kehoe, O. (2021). Therapeutic Effects of Hypoxic and Pro-Inflammatory Priming of Mesenchymal Stem Cell-Derived Extracellular Vesicles in Inflammatory Arthritis. *Int J Mol Sci* , 23 (1). <https://doi.org/10.3390/ijms23010126>
- Kraitchman, D. L., Tatsumi, M., Gilson, W. D., Ishimori, T., Kedziorek, D., Walczak, P., . . . Bulte, J. W. (2005). Dynamic imaging of allogeneic mesenchymal stem cells trafficking to myocardial infarction. *Circulation* , 112 (10), 1451-1461. <https://doi.org/10.1161/CIRCULATIONAHA.105.537480>
- Le Blanc, K., Frassoni, F., Ball, L., Locatelli, F., Roelofs, H., Lewis, I., . . . Marrow, T. (2008). Mesenchymal stem cells for treatment of steroid-resistant, severe, acute graft-versus-host disease: a phase II study. *Lancet* , 371 (9624), 1579-1586. [https://doi.org/10.1016/S0140-6736\(08\)60690-X](https://doi.org/10.1016/S0140-6736(08)60690-X)
- Lembong, J., Kirian, R., Takacs, J. D., Olsen, T. R., Lock, L. T., Rowley, J. A., & Ahsan, T. (2020). Bioreactor Parameters for Microcarrier-Based Human MSC Expansion under Xeno-Free Conditions in a Vertical-Wheel System. *Bioengineering (Basel)* , 7 (3). <https://doi.org/10.3390/bioengineering7030073>
- Ma, J., Zhao, Y., Sun, L., Sun, X., Zhao, X., Sun, X., . . . Zhu, W. (2017). Exosomes Derived from Akt-Modified Human Umbilical Cord Mesenchymal Stem Cells Improve Cardiac Regeneration and Promote Angiogenesis via Activating Platelet-Derived Growth Factor D. *Stem Cells Transl Med* , 6 (1), 51-59. <https://doi.org/10.5966/sctm.2016-0038>
- Madlambayan, G. J., Rogers, I., Kirouac, D. C., Yamanaka, N., Mazurier, F., Doedens, M., . . . Zandstra, P. W. (2005). Dynamic changes in cellular and microenvironmental composition can be controlled to elicit in vitro human hematopoietic stem cell expansion. *Exp Hematol* , 33 (10), 1229-1239. <https://doi.org/10.1016/j.exphem.2005.05.018>
- Malhotra, S., Dumoga, S., Sirohi, P., & Singh, N. (2019). Red Blood Cells-Derived Vesicles for Delivery of Lipophilic Drug Camptothecin. *ACS Appl Mater Interfaces* , 11 (25), 22141-22151.

<https://doi.org/10.1021/acsami.9b04827>

Mawji, I., Roberts, E. L., Dang, T., Abraham, B., & Kallos, M. S. (2022). Challenges and opportunities in downstream separation processes for mesenchymal stromal cells cultured in microcarrier-based stirred suspension bioreactors. *Biotechnol Bioeng* , 119 (11), 3062-3078. <https://doi.org/10.1002/bit.28210>

Mazzini, L., Ferrero, I., Luparello, V., Rustichelli, D., Gunetti, M., Mareschi, K., . . . Fagioli, F. (2010). Mesenchymal stem cell transplantation in amyotrophic lateral sclerosis: A Phase I clinical trial. *Exp Neurol* , 223 (1), 229-237. <https://doi.org/10.1016/j.expneurol.2009.08.007>

Mizukami, A., Fernandes-Platzgummer, A., Carmelo, J. G., Swiech, K., Covas, D. T., Cabral, J. M., & da Silva, C. L. (2016). Stirred tank bioreactor culture combined with serum-/xenogeneic-free culture medium enables an efficient expansion of umbilical cord-derived mesenchymal stem/stromal cells. *Biotechnol J* , 11 (8), 1048-1059. <https://doi.org/10.1002/biot.201500532>

Moon, G. J., Sung, J. H., Kim, D. H., Kim, E. H., Cho, Y. H., Son, J. P., . . . Bang, O. Y. (2019). Application of Mesenchymal Stem Cell-Derived Extracellular Vesicles for Stroke: Biodistribution and MicroRNA Study. *Transl Stroke Res* , 10 (5), 509-521. <https://doi.org/10.1007/s12975-018-0668-1>

Pascucci, L., Cocce, V., Bonomi, A., Ami, D., Ceccarelli, P., Ciusani, E., . . . Pessina, A. (2014). Paclitaxel is incorporated by mesenchymal stromal cells and released in exosomes that inhibit in vitro tumor growth: a new approach for drug delivery. *J Control Release* , 192 , 262-270. <https://doi.org/10.1016/j.jconrel.2014.07.042>

Phinney, D. G., & Pittenger, M. F. (2017). Concise Review: MSC-Derived Exosomes for Cell-Free Therapy. *Stem Cells* , 35 (4), 851-858. <https://doi.org/10.1002/stem.2575>

Prasad, V. K., Lucas, K. G., Kleiner, G. I., Talano, J. A., Jacobsohn, D., Broadwater, G., . . . Kurtzberg, J. (2011). Efficacy and safety of ex vivo cultured adult human mesenchymal stem cells (Prochymal) in pediatric patients with severe refractory acute graft-versus-host disease in a compassionate use study. *Biol Blood Marrow Transplant* , 17 (4), 534-541. <https://doi.org/10.1016/j.bbmt.2010.04.014>

Schop, D., Janssen, F. W., van Rijn, L. D., Fernandes, H., Bloem, R. M., de Bruijn, J. D., & van Dijkhuizen-Radersma, R. (2009). Growth, metabolism, and growth inhibitors of mesenchymal stem cells. *Tissue Eng Part A* , 15 (8), 1877-1886. <https://doi.org/10.1089/ten.tea.2008.0345>

Sotiropoulou, P. A., Perez, S. A., Salagianni, M., Baxevanis, C. N., & Papamichail, M. (2006). Characterization of the optimal culture conditions for clinical scale production of human mesenchymal stem cells. *Stem Cells* , 24 (2), 462-471. <https://doi.org/10.1634/stemcells.2004-0331>

Sun, D., Zhuang, X., Xiang, X., Liu, Y., Zhang, S., Liu, C., . . . Zhang, H. G. (2010). A novel nanoparticle drug delivery system: the anti-inflammatory activity of curcumin is enhanced when encapsulated in exosomes. *Mol Ther* , 18 (9), 1606-1614. <https://doi.org/10.1038/mt.2010.105>

Syromiatnikova, V., Prokopeva, A., & Gomzikova, M. (2022). Methods of the Large-Scale Production of Extracellular Vesicles. *Int J Mol Sci* , 23 (18). <https://doi.org/10.3390/ijms231810522>

Toma, C., Wagner, W. R., Bowry, S., Schwartz, A., & Villanueva, F. (2009). Fate of culture-expanded mesenchymal stem cells in the microvasculature: in vivo observations of cell kinetics. *Circ Res* , 104 (3), 398-402. <https://doi.org/10.1161/CIRCRESAHA.108.187724>

Tsai, A. C., & Pacak, C. A. (2021). Bioprocessing of Human Mesenchymal Stem Cells: From Planar Culture to Microcarrier-Based Bioreactors. *Bioengineering (Basel)* , 8 (7). <https://doi.org/10.3390/bioengineering8070096>

Tsuji, K., Ojima, M., Otabe, K., Horie, M., Koga, H., Sekiya, I., & Muneta, T. (2017). Effects of Different Cell-Detaching Methods on the Viability and Cell Surface Antigen Expression of Synovial Mesenchymal Stem Cells. *Cell Transplant* , 26 (6), 1089-1102. <https://doi.org/10.3727/096368917X694831>

- Viswanathan, S., Shi, Y., Galipeau, J., Krampera, M., Leblanc, K., Martin, I., . . . Sensebe, L. (2019). Mesenchymal stem versus stromal cells: International Society for Cell & Gene Therapy (ISCT(R)) Mesenchymal Stromal Cell committee position statement on nomenclature. *Cytotherapy* , 21 (10), 1019-1024. <https://doi.org/10.1016/j.jcyt.2019.08.002>
- Wang, Y., Lai, X., Wu, D., Liu, B., Wang, N., & Rong, L. (2021). Umbilical mesenchymal stem cell-derived exosomes facilitate spinal cord functional recovery through the miR-199a-3p/145-5p-mediated NGF/TrkA signaling pathway in rats. *Stem Cell Res Ther* , 12 (1), 117. <https://doi.org/10.1186/s13287-021-02148-5>
- Webber, J., & Clayton, A. (2013). How pure are your vesicles? *J Extracell Vesicles* , 2 . <https://doi.org/10.3402/jev.v2i0.19861>
- Witwer, K. W., Soekmadji, C., Hill, A. F., Wauben, M. H., Buzas, E. I., Di Vizio, D., . . . Thery, C. (2017). Updating the MISEV minimal requirements for extracellular vesicle studies: building bridges to reproducibility. *J Extracell Vesicles* , 6 (1), 1396823. <https://doi.org/10.1080/20013078.2017.1396823>
- Zhang, B., Yin, Y., Lai, R. C., Tan, S. S., Choo, A. B., & Lim, S. K. (2014). Mesenchymal stem cells secrete immunologically active exosomes. *Stem Cells Dev* , 23 (11), 1233-1244. <https://doi.org/10.1089/scd.2013.0479>
- Zhou, T., Yuan, Z., Weng, J., Pei, D., Du, X., He, C., & Lai, P. (2021). Challenges and advances in clinical applications of mesenchymal stromal cells. *J Hematol Oncol* , 14 (1), 24. <https://doi.org/10.1186/s13045-021-01037-x>
- Zhu, L. P., Tian, T., Wang, J. Y., He, J. N., Chen, T., Pan, M., . . . Bai, Y. P. (2018). Hypoxia-elicited mesenchymal stem cell-derived exosomes facilitates cardiac repair through miR-125b-mediated prevention of cell death in myocardial infarction. *Theranostics* , 8 (22), 6163-6177. <https://doi.org/10.7150/thno.28021>